IEEE Access
Multidisciplinary | Rapid Review | Open Access Journal

Received August 23, 2020, accepted September 2, 2020, date of publication September 7, 2020,
date of current version September 21, 2020.

Digital Object Identifier 10.1109/ACCESS.2020.3022595

Comparative Study on Variable Flux Memory Machines With Different Arrangements of Permanent Magnets

YING XIE, (Senior Member, IEEE), ZHAOYANG NING, AND ZEXIN MA
School of Electrical and Electronic Engineering, Harbin University of Science and Technology, Harbin 150080, China

Corresponding author: Zhaoyang Ning (ningzhaoyang@hrbust.edu.cn)

This work was supported by the National Natural Science Foundation of China under Grant 51977052.

ABSTRACT Compared with conventional permanent magnet synchronous motor, variable flux memory motor (VFMM) possesses the advantage of adjusting the magnetization state online. Because of its wide speed range and large high-efficiency region, it becomes a competitive candidate for the electric drive system. This paper presents a novel parallel hybrid magnets VFMM which is obtained by updating a conventional series hybrid permanent magnets VFMM. The proposed motor adopts a new permanent magnet arrangement and the combination of low coercive force permanent magnet and high coercive force permanent magnet is used. The proposed parallel hybrid permanent magnets VFMM and the series hybrid permanent magnets VFMM are compared. The equivalent magnetic circuit models of the motors are used to explain the principle of the motors. The finite element analysis method is used to study the fundamental properties, such as open circuit radial flux density, unintentional demagnetization with q-axis current, intentional demagnetization with d-axis current, torque capability, and efficiency characteristics. It was shown the efficiency of the parallel hybrid permanent magnets VFMM is higher in the high-speed region and the magnetization state adjustment range of the parallel hybrid permanent magnets VFMM is larger.

INDEX TERMS Equivalent magnetic circuit, hybrid permanent magnet, magnetization state, variable flux memory motor.

I. INTRODUCTION

VARIABLE flux memory motor (VFMM) is a class of permanent magnet motor with the ability to change magnetization state and memorize the flux density of the magnets in motors [1]–[4]. VFMM is equipped with low coercive force permanent magnet, for example, AlNiCo, SmCo, and Ferrite [5], [6]. Due to the unique advantage of the property to regulate the magnetization state by applying a current pulse when the motor is running, VFMM shows the typical speed-torque characteristic required for the electric drive system. The motor is needed to provide high torque while the electric vehicle is climbing or accelerating [7]. For this operation condition, VFMM keeps its magnetization state at a high level to provide the high torque. While the electric vehicle driving at high speed, the motor is required to run at a high speed too. Because of the inverter voltage limitation, the conventional permanent magnet synchronous motor needs to use the flux weakening control strategy to increase the speed. VFMM can regulate the magnetization state to keep it at a low level, it will increase the speed without a negative d-axis flux weakening current, and therefore the risk of irreversible demagnetization of the permanent magnet is reduced. Same as the electrically excited motor, VFMM can adjust the magnetization state online. It has attracted the attention of researchers all over the world and is regarded as a great choice for the electric drive system [8]. Recently, scholars all over the world have done a lot of research on VFMM [9], [10]. A variable flux intensifying interior permanent magnet motor used AlNiCo is proposed in [11], the magnets are tangentially magnetized and big q-axis barriers are inserted in the rotor to provide reluctance torque with positive d-axis current. The influence of different design parameters on the required current of remagnetizing the magnets is studied in [12]. However, the torque ripple of the tangentially magnetized motor is larger than the conventional permanent magnet synchronous motor. An uneven air-gap is adopted by [6] and this method is demonstrated to

The associate editor coordinating the review of this manuscript and approving it for publication was Jinquan Xu.

be helpful to reduce torque ripple by finite element analysis. In [13], a motor equipped with the permanent magnets which are magnetized to the different magnetization state level is studied. By means of comparing the efficiency maps of the motor with the different magnetization state level, the optimal efficiency map is achieved. Some consequent-pole VFMMs are studied in some papers [14], [15]. The low coercive force permanent magnets are replaced by iron or soft magnetic composites. The air-gap flux is provided by two components, one is constant provided by permanent magnets, another is provided by the field winding.

However, the torque density of a motor equipped with low coercive force permanent magnets is usually low. Hybrid permanent magnets VFMM equipped with high coercive force permanent magnets and low coercive force permanent magnets has been investigated in some research. High coercive force permanent magnets guarantee to provide high torque, and low coercive force permanent magnets keep the property of regulating the magnetization state. A flux-variable partitioned stator permanent magnet claw pole motor is proposed in [16], the relationship between the thickness of permanent magnets and the largest linear control range of the gap flux density is found. A parallel hybrid permanent magnets VFMM is proposed in [17], the high coercive force permanent magnets are tangentially set, and the low coercive force permanent magnets are radially set. Another parallel hybrid permanent magnets VFMM is proposed in [18]. Especially, magnetic barriers are inserted in the rotor to solve the problem proposed in [19]. Due to the cross-coupling effect, the magnetization state of low coercive force permanent magnets will be unstable, because the high coercive force permanent magnets apply a demagnetization effect on low coercive force permanent magnets. A hybrid permanent magnets VFMM with arc-shaped magnets is proposed in [20], these magnets can help increase magnet torque and reluctance torque. A VFMM with series hybrid permanent magnets is proposed in [21]. Because the high coercive force permanent magnets and the low coercive force permanent magnets are connected in series, the high coercive force permanent magnets help the low coercive force permanent magnets to resist the demagnetization induced by the armature reaction. The comparison of the VFMMs with series and parallel hybrid permanent magnets is investigated elaborately in [22], the conclusion shows that the VFMM with series hybrid permanent magnets has a more stable operation point and higher torque density. However, the capability of weakening the magnetization state of the VFMM with series hybrid permanent magnets is worse than the VFMM with parallel hybrid permanent magnets.

In order to increase the magnetization state adjustment range, a novel VFMM with parallel hybrid permanent magnets is proposed in this paper. A combination of the thin permanent magnet with high coercive force and the thick permanent magnet with low coercive force is adopted. The proposed parallel hybrid permanent magnets VFMM and the series hybrid permanent magnets VFMM are compared to identify their different features, which could offer a guideline for motor designers. In order to explain the operating principle of the motors, the equivalent magnetic circuit models are established. Finite element simulations are used to compare the electromagnetic performance of these two motors.

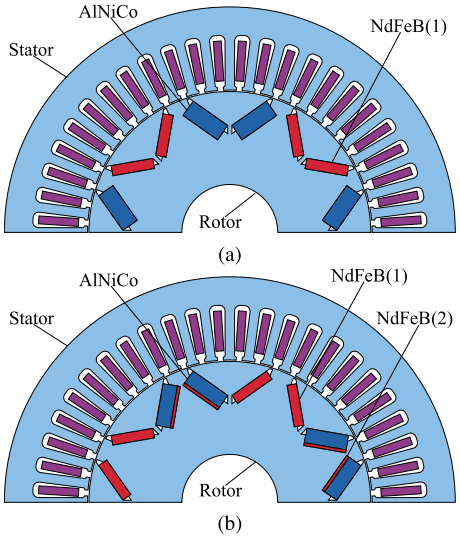

FIGURE 1. Structures of motors. (a) Series hybrid permanent magnets VFMM. (b) Parallel hybrid permanent magnets VFMM.

II. MOTOR STRUCTURE AND OPERATING PRINCIPLE

A motor that is suitable for electric drive systems is proposed in this paper. The structure of the proposed parallel hybrid permanent magnets VFMM is shown in Fig. 1b, which is obtained by updating a series hybrid permanent magnets VFMM as shown in Fig. 1a. The combination of AlNiCo and NdFeB is adopted because the coercive force of AlNiCo is so low that it will be demagnetized easily. When an interior permanent magnet synchronous motor equipped with AlNiCo operates at the high torque region, it is hard for the motor to provide enough reluctance torque, because a large negative d-axis current will demagnetize the AlNiCo. In fact, even an Id=0 control strategy is applied to the VFMM, because of the low coercive force, the AlNiCo may also be demagnetized caused by q-axis current. In order to overcome the shortcoming of the low coercive force of AlNiCo, the combination of AlNiCo and thin NdFeB is adopted to replace the original AlNiCo. The required magnetic properties can be obtained by adjusting the thickness of the two different kinds of permanent magnets. These two motors have the same dimensions which are designed based on a commercial interior permanent magnet motor which is applied in an electric vehicle. In order to compare the performance of the two motors fairly, the volume of permanent magnets is also the same in these two motors. The difference between these two motors is the arrangement of the permanent magnets. The key design parameters of the two motors are listed in Table. 1.

In order to illustrate the features of the proposed motor clearly, the equivalent magnetic circuits under the no-load condition of the series and parallel hybrid permanent magnets

TABLE 1. Key design parameters of the series and parallel hybrid permanent magnets VFMMs.

Parameter	Parallel hybrid	Series hybrid
Phase number	3	3
Stator slot/pole number	48/8	48/8
Axial length	150mm	150mm
Stator outer diameter	160mm	160mm
Stator inner diameter	101mm	101mm
Rotor outer diameter	100mm	100mm
AlNiCo thickness	6mm	6mm
NdFeB(1) thickness	**3.5mm**	**3.7mm**
NdFeB(2) thickness	**0.2mm**	
AlNiCo width	30mm	30mm
NdFeB width	30mm	30mm
AlNiCo Br	1.05T	1.05T
NdFeB Br	1.125T	1.125T
AlNiCo Hc	112kA/m	112kA/m
NdFeB Hc	895kA/m	895kA/m
Rated current	180A	180A

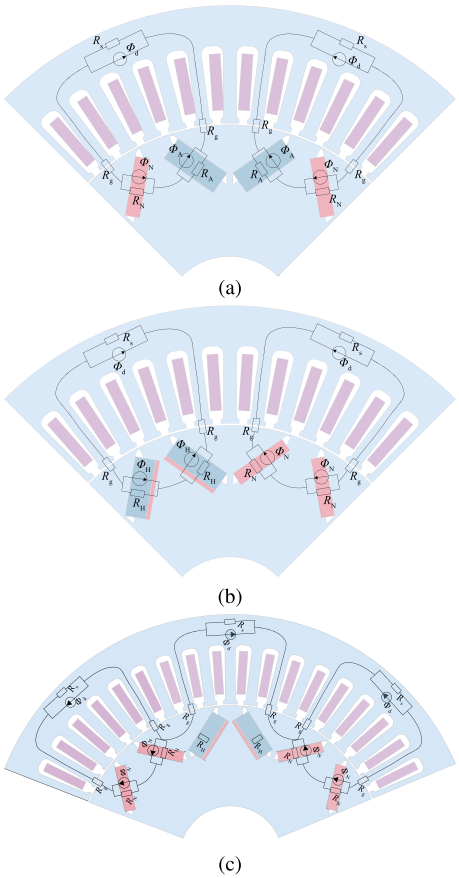

FIGURE 2. Equivalent magnetic circuits of the motors under no-load condition. (a) Series hybrid permanent magnets VFMM. (b) Parallel hybrid permanent magnets VFMM. (c) Parallel hybrid permanent magnets VFMM with full demagnetization.

VFMMs are demonstrated in Fig. 2. For a VFMM, the d-axis current adjusts the magnetization state online. Φ_N, Φ_A, Φ_H, and Φ_d are fluxes provided by NdFeB, AlNiCo, combination of NdFeB and AlNiCo, and d-axis stator current respectively. R_N, R_A, R_H, R_g, and R_S are the reluctances of NdFeB, AlNiCo, the combination of NdFeB and AlNiCo, air-gap, and stator respectively. As shown in the Fig. 2b, the magnetic circuits of the parallel hybrid permanent magnets VFMM is asymmetrical but the magnetic circuits of the series hybrid permanent magnets VFMM is symmetrical as shown in Fig. 2a. The equivalent magnetic circuit of the parallel hybrid permanent magnets VFMM, when one side is demagnetized, is shown in Fig. 2c. When the AlNiCo is fully demagnetized, NdFeB provides all the fluxes and the effective d-axis of the motor does not move.

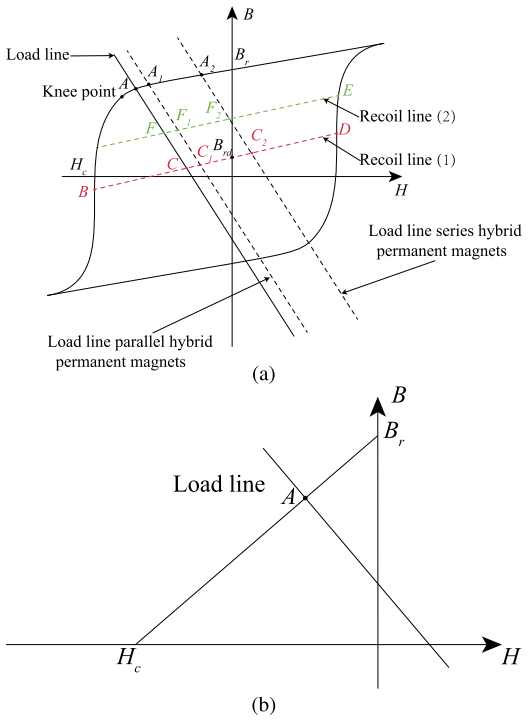

FIGURE 3. Illustration of operation point of permanent magnet (B: flux density, H: magnetic field strength). (a) AlNiCo. (b) NdFeB.

The dynamic regulation principles of the operation point of AlNiCo and NdFeB are shown in Fig. 3a and Fig. 3b. The coercive force of AlNiCo is relatively low, and the knee point of AlNiCo is higher than NdFeB. In fact, the demagnetization curve of NdFeB is nearly linear in quadrant II. Usually, because of the low coercive force of AlNiCo, it is easy to change the magnetization state of it. For example, while a negative d-axis pulse current is applied, the generated negative magnetomotive force will push the operation point from initial point A slides to point B. After the negative current is released, the operation point moves to point C along the recoil line (1). The corresponding new remanent flux density B_{rd} is shown in Fig. 3a, and the magnetization state MS is defined as follows:

$$MS = \frac{B_{rd}}{B_r} \tag{1}$$

If a positive d-axis pulse current is applied, a positive magnetomotive force will push the operation point moves along *CDE* and then settles at point *F* after the positive current is released. On the contrary, the operation point of NdFeB will not change while changing the d-axis current.

However, in the series hybrid permanent magnets VFMM, every magnetic circuit contains Φ_N and Φ_A, and they are connected in series. Due to the high coercive of NdFeB, the operation point of AlNiCo will settle at points A_2, C_2, and F_2 which are higher than points A, C, and F as shown in Fig. 3a. It will reduce the magnetization state adjustment range of the AlNiCo.

Differently, there are two different kinds of magnetic circuits in the parallel hybrid permanent magnets VFMM and Fig. 2b shows a quarter motor model. In the first kind of magnetic circuit, the flux Φ_H consists of the combination of NdFeB and AlNiCo, and the NdFeB is thin. The operation point will settle at points A_1, C_1, and F_1 which are lower than points A_2, C_2, and F_2. So, the magnetization state adjustment range of the parallel hybrid permanent magnets VFMM is larger than the series hybrid permanent magnets VFMM. The flux Φ_N in the second kind magnetic circuit is fixed, it provides a stable magnetic field.

III. ELECTROMAGNETIC PERFORMANCE COMPARISON

In this section, the electromagnetic performance of the series and parallel hybrid permanent magnets VFMMs are comprehensively compared by finite element simulations.

A. OPEN CIRCUIT RADIAL FLUX DENSITY

Fig. 4 and Fig. 5 shows the no-load radial air-gap flux densities comparison, where Fig. 5a and Fig. 4a show the waveform comparison when the magnetization state is 100% and 0% respectively, Fig. 4b and Fig. 5b show the harmonic spectra comparison when the magnetization state is 100% and 0%. When the magnetization state is 0%, the fundamental amplitude of the air-gap flux density of the parallel hybrid permanent magnets VFMM is smaller. So the proposed parallel hybrid permanent magnets VFMM has a wider flux variation range.

B. UNINTENTIONAL DEMAGNETIZATION WITH Q-AXIS CURRENT

The demagnetization caused by the q-axis current may occur in the memory motor, which will reduce the output torque. In order to compare the demagnetization caused by the q-axis current, finite element simulations are carried out following these processes. Firstly, freeze the magnetization state of all permanent magnets under the rated load and then perform a no-load simulation. According to the formula of no-load back electromotive force(EMF):

$$e = 4.44 f N K_w \Phi \tag{2}$$

where f is the frequency of the stator current, N is the number of turns of per phase winding, K_w is the winding factor, and Φ is the amplitude of air-gap flux. The magnetization

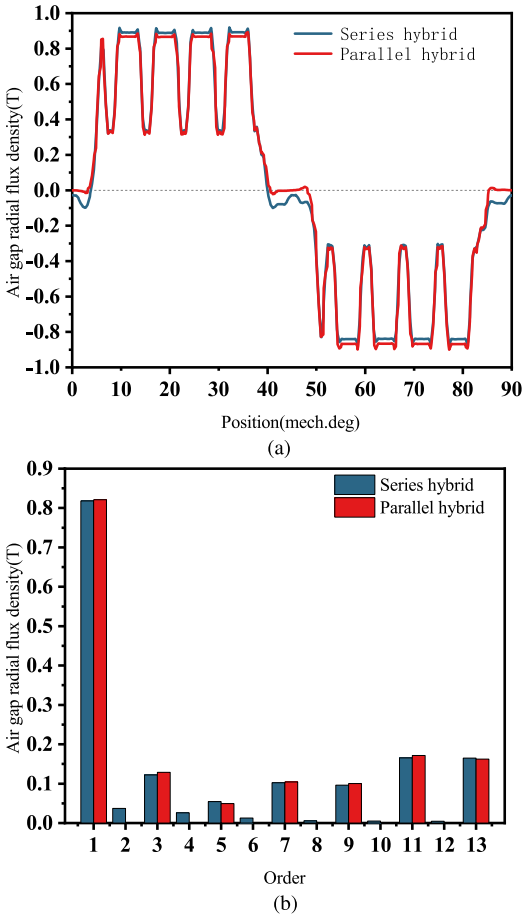

FIGURE 4. No-load air-gap radial flux densities while magnetization state is 100%. (a) Waveforms. (b) Harmonic spectra.

state of the permanent magnet can be judged based on the waveform of the back EMF. The results are shown in Fig. 6, when the current is less than 100A, there is basically no demagnetization caused by the q-axis current in both motors, but when the current is larger than 100A, demagnetization occurs in both motors, and the demagnetization in the parallel hybrid permanent magnets VFMM is more serious. When the q-axis current is 200A, the demagnetization rate is 18% in the parallel hybrid permanent magnets VFMM and 8% in the series hybrid permanent magnets VFMM.

C. INTENTIONAL DEMAGNETIZATION WITH D-AXIS CURRENT

The magnetization state of the memory motor can be adjusted in real-time by applying d-axis current. The no-load back EMF amplitudes after applying different d-axis current are shown in Fig. 7. When the demagnetization current is 325A, the no-load back EMF of the parallel hybrid permanent magnets VFMM and the series hybrid permanent magnets VFMM is 0.5V and 70.5V, and the variable rate is shown in Table. 2. After applying the 325A demagnetization current, the RMS values of the no-load back EMFs of the series and parallel hybrid permanent magnets VFMMs decrease by 34.6% and 99.53% respectively. It shows that the magnetization state

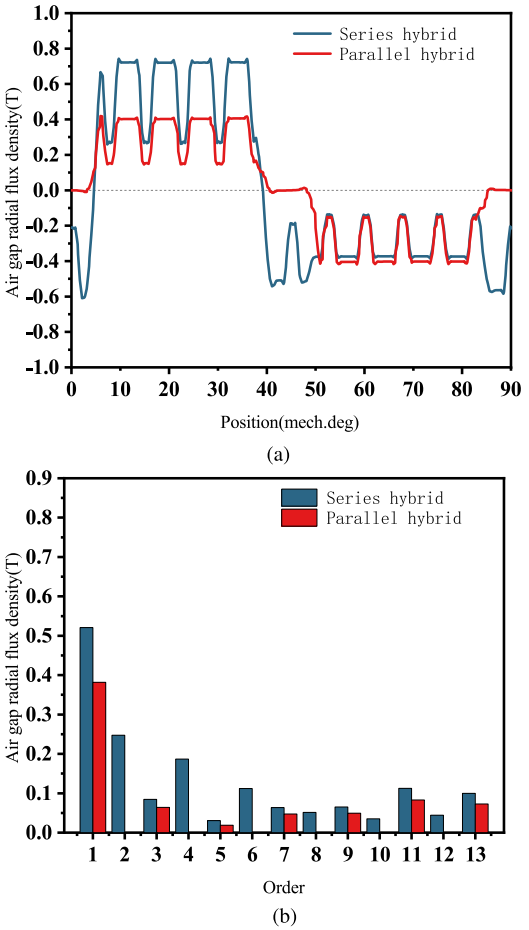

FIGURE 5. No-load air-gap radial flux densities while magnetization state is 0%. (a) Waveforms. (b) Harmonic spectra.

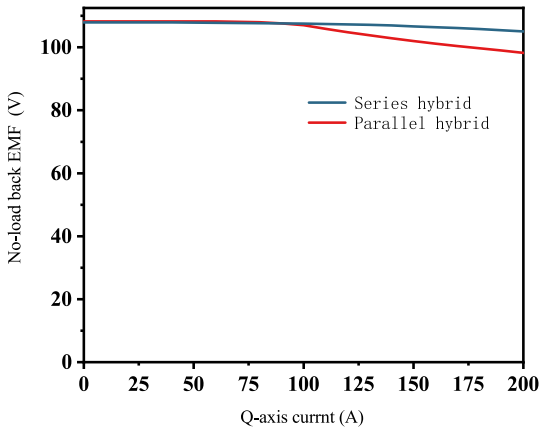

FIGURE 6. Unintentional demagnetization due to q-axis current.

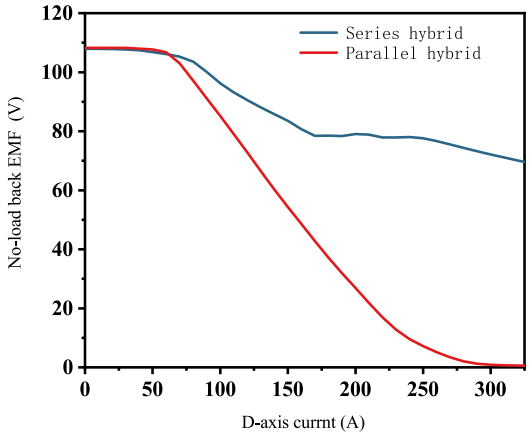

FIGURE 7. Intentional demagnetization due to d-axis current.

TABLE 2. No-load back EMFs before and after applying 325A d-axis current in the parallel and series hybrid permanent magnets VFMMs.

Parameter	Prallel hybrid	Series hybrid
RMS value of no-load back EMF before demagnetization	108.2V	107.9V
RMS value of no-load back EMF after applying 325A d-axis current	0.5V	70.5V
Variable rate	99.53%	34.6%

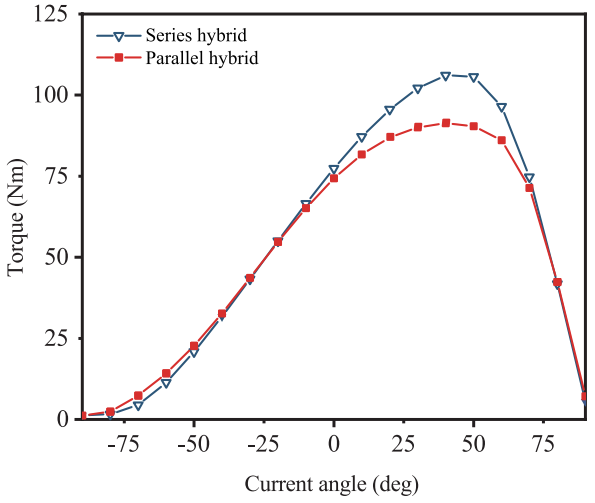

FIGURE 8. Relationship between the current angle and the output torque of the series and parallel hybrid permanent magnets VFMMs.

adjustment range of the AlNiCo in the parallel hybrid permanent magnets VFMM is wider a lot. As a result, the parallel hybrid permanent magnets VFMM has a wider speed range.

D. TORQUE CAPABILITY

The torque capabilities of the series and parallel hybrid permanent magnets VFMMs are investigated. The relationship between the current angle and the output torque while inputting 180A current is shown in Fig. 8. While setting the current angle to be 40deg, these two motors provide the maximum torque. The maximum output torque of the series and parallel hybrid permanent magnets VFMMs is 106.08Nm and 89.89Nm respectively. The comparison of torque ripple while the current is 180A and the current angle is 40deg is shown in Fig. 9. The results show that the torque ripple

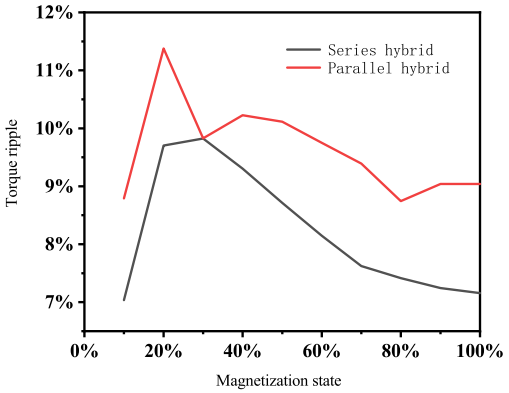

FIGURE 9. Torque ripple of the series and parallel hybrid permanent magnets VFMMs.

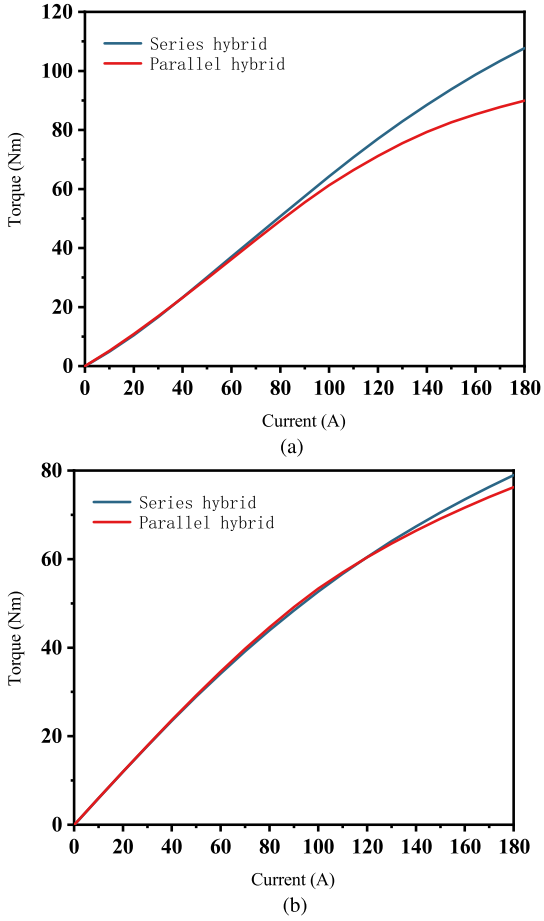

FIGURE 10. Relationship between the current amplitudes and the output torque of the series and parallel hybrid permanent magnets VFMMs. (a) Current angle of 40 deg. (b) Current angle of 0 deg.

of the series hybrid permanent magnets VFMM is smaller than that of the parallel hybrid permanent magnets VFMM. Furthermore, the relationship between the current amplitudes and the output torque while the current angle is 40 deg and 0deg are shown in Fig. 10 and Fig. 10b.

The relation of the output torque, the permanent magnet torque, and the reluctance torque of an interior permanent magnet motor can be expressed as [23]:

$$T = T_{PM} + T_{RM} \tag{3}$$

$$T_{PM} = \frac{3}{2} p \psi_f I_q \tag{4}$$

$$T_{RM} = \frac{3}{2} p (L_d - L_q) I_d I_q \tag{5}$$

where T, T_{PM}, T_{RM}, p, ψ_f, I_q, I_d, L_q, and L_d are the output torque, the permanent magnet torque, the reluctance torque, the rotor pole pair number, the permanent magnet flux linkage, the q-axis current, the d-axis current, the q-axis inductance, and the d-axis inductance. While the current angle is 0deg, these two motors only provide permanent magnet torque. While the current angle is 40deg, these two motors provide permanent magnet torque and reluctance torque. So these two motors have a similar ability to provide permanent magnet torque, but the ability of the series hybrid permanent magnets VFMM to provide reluctance torque is better.

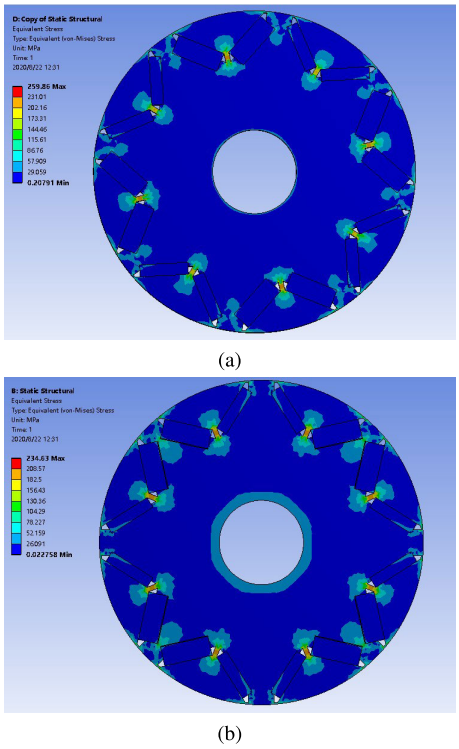

FIGURE 11. Rotor stress distributions. (a) Series hybrid permanent magnets VFMM. (b) Parallel hybrid permanent magnets VFMM.

E. ROTOR STRESS AND THERMAL CONDITION

The rotor stress distributions of the two motors are shown in Fig. 11. While the motor speed is 20000 rpm, the maximum rotor stress of the series hybrid permanent magnets VFMM is 259.86 MPa and the maximum rotor stress of the parallel hybrid permanent magnets VFMM is 234.63 MPa. The maximum allowed yield strength of the rotor core is 280 MPa. Although the speed of the motors is high, the maximum stress of the rotors still meets the requirements, and the structural design of the rotors is reasonable.

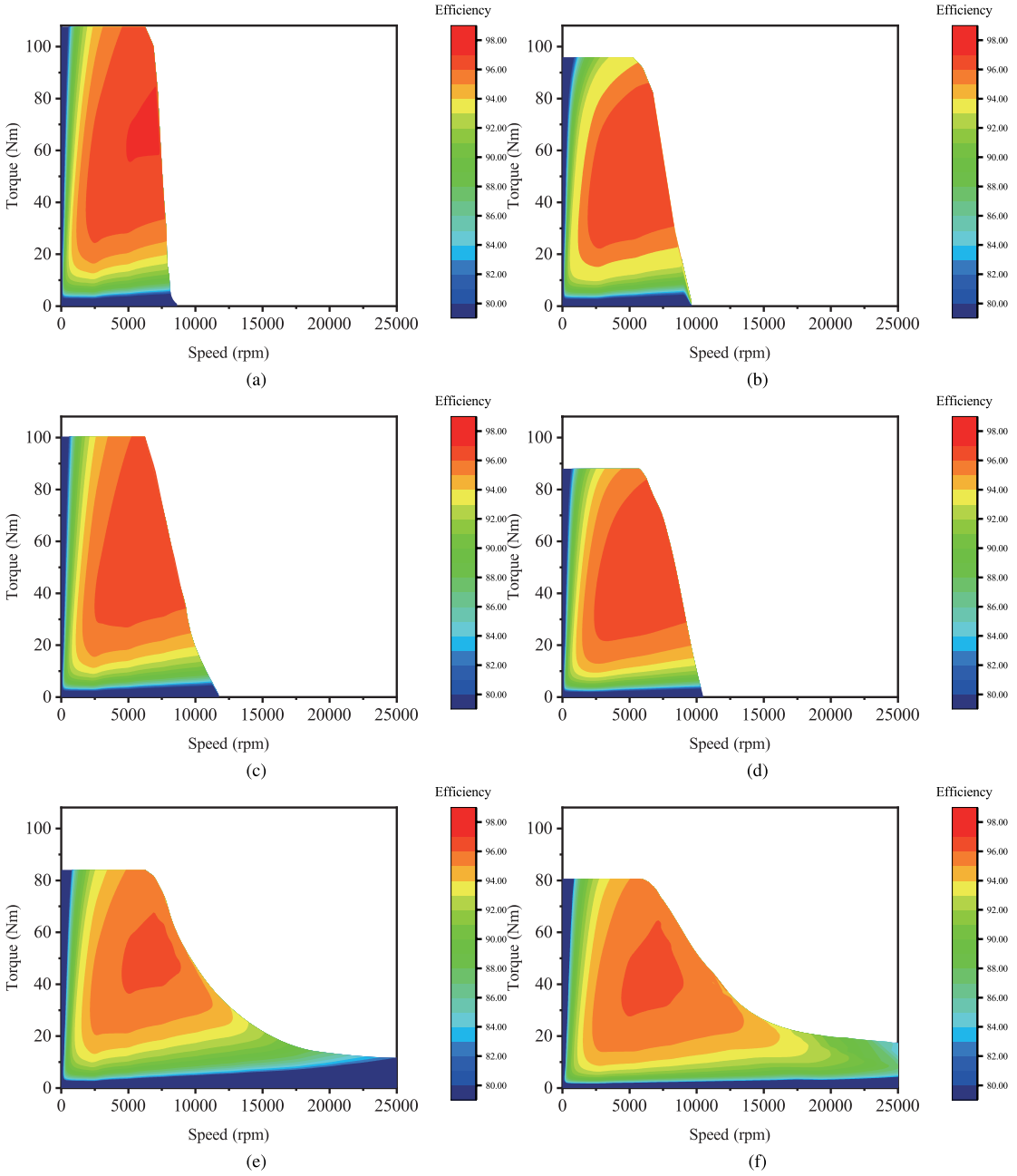

FIGURE 12. Efficiency map. (a) The series hybrid permanent magnets VFMM while magnetization state is 100%. (b) The parallel hybrid permanent magnets VFMM while magnetization state is 100%. (c) The series hybrid permanent magnets VFMM while magnetization state is 60%. (d) The parallel hybrid permanent magnets VFMM while magnetization state is 60%. (e) The series hybrid permanent magnets VFMM while magnetization state is 10%. (f) The parallel hybrid permanent magnets VFMM while magnetization state is 10%.

The temperature of each part of the motor has an important impact on the motor. Due to the high current density of the two motors, water cooling is adopted. The temperature of the two motors after they stabilize at the rated operation point are shown in Table. 3. The temperature of each part in the parallel hybrid permanent magnets VFMM is higher than that of the series hybrid permanent magnets VFMM, but the temperature of each part of the two motors is within the allowable value.

TABLE 3. The temperature of each part of the series and parallel hybrid permanent magnets VFMMs.

Part	Parallel hybrid	Series hybrid
Armature winding	105.8 °C	99.21 °C
Magnet	110.4 °C	103.42 °C
Stator	102.7 °C	95.6 °C
Rotor	100.7 °C	92.84 °C
Shaft	98.9 °C	91.63 °C

F. EFFICIENCY CHARACTERISTICS

Generally, in the vehicle electric drive system, the motor control strategy is a combination of maximum torque per ampere (MTPA) and flux weakening control. When the motor operates below the base speed, the MTPA control strategy is adopted, and the motor is switched to flux weakening control strategy when the speed is higher than the base speed [24].

It is completely different. Compared with the conventional permanent magnet synchronous motor, the most significant feature of the VFMM is that it can adjust the magnetization state of low coercive force permanent magnets online. So the control method of VFMM is more complicated than that of permanent magnet synchronous motor. For the VFMM, when the motor speed is higher than the base speed, the magnetization state of the low coercive force permanent magnets in the motor should be reduced first, instead of using the flux weakening control strategy until the magnetization state is minimized. If the speed needs to be further increased, the flux weakening control strategy should be adopted.

The efficiency maps of the two motors at different magnetization state levels are investigated. While the magnetization state is 100% or 60%, the MTPA control strategy is adopted, and the flux weakening control strategy is adopted when the magnetization state is 10%. As shown in Fig. 12a, Fig. 12b, Fig. 12c, and Fig. 12d, under the condition of maintaining the same magnetization state level, the maximum torque of the series hybrid permanent magnets VFMM is higher than that of the parallel hybrid permanent magnets VFMM, and the efficiency of series hybrid permanent magnets VFMM in the high torque region is also higher than that of the parallel hybrid permanent magnets VFMM. The reason is that series hybrid permanent magnets VFMM can produce larger reluctance torque. But the speed range of the parallel hybrid permanent magnets VFMM is wider than the series hybrid permanent magnets VFMM. It can be seen from Fig. 12e and Fig. 12f, the maximum output torque of the two motors is almost equal and the high-efficiency region of the parallel hybrid permanent magnets VFMM is wider. Especially in the high-speed region, the efficiency advantage is particularly significant.

TABLE 4. Key speed-torque points selected according to the worldwide harmonized light duty test cycle.

Operation point	Speed	Torque
Point A	2000rpm	23Nm
Point B	4000rpm	70Nm
Point C	6000rpm	18Nm
Point D	8000rpm	25Nm
Point E	15000rpm	15Nm
Point F	20000rpm	12Nm

In order to compare the losses of the two motors for duty cycle applications, several key operation points are selected according to the worldwide harmonized light duty test cycle. These points are shown in Table. 4. The winding temperature is assumed to be stable at 60°C and the results are presented in Fig. 13. When the motors operate at thee high-torque region, the copper loss is high and when the motors operate at the high-speed region the iron loss is high. It can be seen that in the middle-speed and low-speed region, the losses of the two motors are similar, but in the high-speed region, the iron losses of the parallel hybrid permanent magnets VFMM reduce by 44.5% and 53.8% at point E and point F. The iron loss of the parallel hybrid permanent magnets VFMM in the high-speed region has a huge advantage.

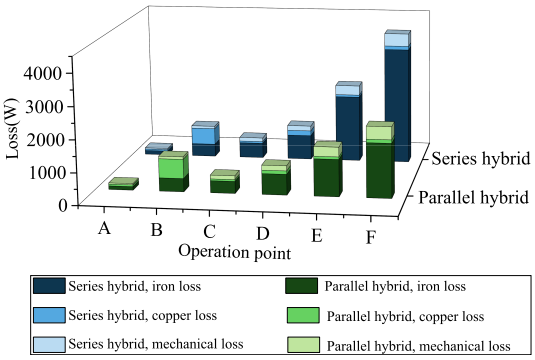

FIGURE 13. Loss distribution at key points selected according to the worldwide harmonized light duty test cycle.

IV. CONCLUSION

Under the condition of keeping the same material cost, a novel parallel hybrid permanent magnets VFMM is proposed by updating a series hybrid permanent magnets VFMM. The combination of low coercive force permanent magnet and high coercive force permanent magnet is used in the parallel hybrid permanent magnets VFMM. Simulation results prove the effectiveness of the methods proposed in this paper. The combination of AlNiCo and NdFeB can enhance the operation point of AlNiCo and increase the utilization rate of it. Compared with the series hybrid permanent magnets VFMM, unintentional demagnetization caused by q-axis current is larger in the parallel hybrid permanent magnets VFMM and the maximum torque of the parallel hybrid permanent magnets VFMM is smaller than the series hybrid permanent magnets VFMM. However, the parallel hybrid permanent magnets VFMM has a wider range of magnetization state adjustment than the series hybrid permanent magnets VFMM. In the middle-speed and low-speed region, the losses of the two motors are similar, but in the high-speed region, the losses of the parallel hybrid permanent magnets VFMM are almost half that of the series hybrid permanent magnets VFMM. The parallel hybrid permanent magnets VFMM is the ideal candidate for the electric drive system. Both motors have their own advantages and disadvantages, designers can make a trade-off choice according to actual application.

REFERENCES

[1] V. Ostovic, "Memory motors," *IEEE Ind. Appl. Mag.*, vol. 9, no. 1, pp. 52–61, Jan. 2003.

[2] W. Wang, H. Lin, H. Yang, W. Liu, and S. Lyu, "Second-order sliding mode-based direct torque control of variable-flux memory machine," *IEEE Access*, vol. 8, pp. 34981–34992, 2020.
[3] R. Jayarajan, N. Fernando, and I. U. Nutkani, "A review on variable flux machine technology: Topologies, control strategies and magnetic materials," *IEEE Access*, vol. 7, pp. 70141–70156, 2019.
[4] J. Chen, H. Fang, and R. Qu, "Online magnetization trajectory prediction and current control for a variable-flux permanent magnet machine," *IEEE Access*, vol. 8, pp. 41325–41334, 2020.
[5] A. Athavale, K. Sasaki, B. S. Gagas, T. Kato, and R. D. Lorenz, "Variable flux permanent magnet synchronous machine (VF-PMSM) design methodologies to meet electric vehicle traction requirements with reduced losses," *IEEE Trans. Ind. Appl.*, vol. 53, no. 5, pp. 4318–4326, Sep. 2017.
[6] A. Sun, J. Li, R. Qu, J. Chen, and H. Lu, "Rotor design considerations for a variable-flux flux-intensifying interior permanent magnet machine with improved torque quality and reduced magnetization current," in *Proc. IEEE Energy Convers. Congr. Expo. (ECCE)*, Sep. 2015, pp. 784–790.
[7] N. Matsui, "Design and control of variable field permanent magnet motors," *IEEJ Trans. Electr. Electron. Eng.*, vol. 14, no. 7, pp. 966–981, Jul. 2019.
[8] M. Wang, C. Tong, P. Zheng, L. Cheng, S. Zhang, G. Qiao, and Y. Sui, "Analysis of a novel hybrid-PM variable-flux machine using new magnet material CeFeB," *IEEE Trans. Magn.*, vol. 55, no. 7, pp. 1–7, Jul. 2019.
[9] H. Yang, Z. Q. Zhu, H. Lin, and W. Chu, "Flux adjustable permanent magnet machines: A technology status review," *Chin. J. Elect. Eng.*, vol. 2, no. 2, pp. 14–30, Dec. 2016.
[10] H. Yang, H. Lin, and Z. Q. Zhu, "Recent advances in variable flux memory machines for traction applications: A review," *CES Trans. Electr. Mach. Syst.*, vol. 2, no. 1, pp. 34–50, Mar. 2018.
[11] M. Ibrahim and P. Pillay, "Design of high torque density variable flux permanent magnet machine using alnico magnets," in *Proc. IEEE Energy Convers. Congr. Expo. (ECCE)*, Sep. 2014, pp. 3535–3540.
[12] M. Ibrahim, L. Masisi, and P. Pillay, "Design of variable flux permanent-magnet machine for reduced inverter rating," *IEEE Trans. Ind. Appl.*, vol. 51, no. 5, pp. 3666–3674, Sep. 2015.
[13] A. Sun, J. Li, R. Qu, B. Zhao, D. Li, H. Fang, and Y. Sun, "Magnetization and performance analysis of a variable-flux flux-intensifying interior permanent magnet machine," in *Proc. IEEE Int. Electr. Mach. Drives Conf. (IEMDC)*, May 2015, pp. 369–375.
[14] J. A. Tapia, F. Leonardi, and T. A. Lipo, "Consequent-pole permanent-magnet machine with extended field-weakening capability," *IEEE Trans. Ind. Appl.*, vol. 39, no. 6, pp. 1704–1709, Nov. 2003.
[15] T. Ogawa, T. Takahashi, M. Takemoto, S. Ogasawara, and A. Daikoku, "The examination of pole geometry of consequent pole type ferrite PM axial gap motor with field winding," in *Proc. IEEE Int. Electr. Mach. Drives Conf. (IEMDC)*, May 2017, pp. 1–7.
[16] J. Hu, Y. Chen, F. Wei, M. Zhao, and X. Ran, "Study on magnetic field regulation of a flux-variable partitioned stator permanent magnet claw pole motor," in *Proc. 22nd Int. Conf. Electr. Mach. Syst. (ICEMS)*, Aug. 2019, pp. 1–5.
[17] C. Yiguang, P. Wei, W. Ying, T. Renyuan, and W. Jing, "Interior composite-rotor controllable-flux PMSM–memory motor," in *Proc. Int. Conf. Electr. Mach. Syst.*, vol. 1, 2005, pp. 446–449.
[18] Y. Zhou, Y. Chen, and J.-X. Shen, "Analysis and improvement of a hybrid permanent-magnet memory motor," *IEEE Trans. Energy Convers.*, vol. 31, no. 3, pp. 915–923, Sep. 2016.
[19] D. Wu, Z. Q. Zhu, T. Sasaki, X. Liu, R. Deodhar, and A. Pride, "Cross coupling effect in hybrid magnet memory motor," in *Proc. 7th IET Int. Conf. Power Electron., Mach. Drives (PEMD)*, 2014, pp. 1–6.
[20] S. Kaneko, T. Yuasa, I. Miki, and Y. Okamoto, "A new variable-field motor with wide range of speed," in *Proc. Int. Symp. Power Electron., Electr. Drives, Autom. Motion (SPEEDAM)*, Jun. 2018, pp. 1131–1135.
[21] H. Hua, Z. Q. Zhu, A. Pride, R. P. Deodhar, and T. Sasaki, "A novel variable flux memory machine with series hybrid magnets," *IEEE Trans. Ind. Appl.*, vol. 53, no. 5, pp. 4396–4405, Sep. 2017.
[22] H. Hua, Z. Q. Zhu, A. Pride, R. Deodhar, and T. Sasaki, "Comparative study on variable flux memory machines with parallel or series hybrid magnets," *IEEE Trans. Ind. Appl.*, vol. 55, no. 2, pp. 1408–1419, Mar. 2019.
[23] T. M. Jahns, G. B. Kliman, and T. W. Neumann, "Interior permanent-magnet synchronous motors for adjustable-speed drives," *IEEE Trans. Ind. Appl.*, vol. IA-22, no. 4, pp. 738–747, Jul. 1986.
[24] X. Gu, T. Li, X. Li, G. Zhang, and Z. Wang, "An improved UDE-based flux-weakening control strategy for IPMSM," *Energies*, vol. 12, no. 21, p. 4077, Oct. 2019.

YING XIE (Senior Member, IEEE) was born in Heilongjiang, China. She received the Ph.D. degree in electric machine and apparatus from the Harbin Institute of Technology, Harbin, China, in 2008. From 2010 to 2012, she held a post-doctoral position with the Huazhong University of Science and Technology, Wuhan, China. She was a Visiting Scholar with Sheffield University, U.K., in 2013. She is currently a Professor with the Harbin University of Science and Technology. Her current research interests include comprehensive physical field calculation, including vibration characteristic and noise applied to electric motor, state monitoring and fault diagnosis of induction motors, and permanent magnet compound motor and drives for new energy electric vehicles.

ZHAOYANG NING was born in Heilongjiang, China, in 1994. He received the B.Eng. degree in electrical engineering from the Harbin University of Science and Technology, Harbin, China, in 2017, where he is currently pursuing the M.Eng. degree. His research interests include synchronous machine topologies and optimization.

ZEXIN MA was born in Heilongjiang, China, in 1993. He received the B.Eng. degree in electrical engineering from the Harbin University of Science and Technology, Harbin, China, in 2017, where he is currently pursuing the M.Eng. degree. His research interests include motor design and the NVH research of motors.